1965MmSAI..36..331A

SPECTROGRAPHIC OBSERVATIONS OF ZETA TAURI FROM 1961 TO 1964

Nota (**) di C. AYDIN (*), M. HACK, S. İŞLIK (*)
(*Osservatorio Astronomico di Trieste*)

Riassunto. — Si danno i risultati delle osservazioni spettrografiche di ζ Tauri nelle tre epoche: 16 novembre 1961-26 marzo 1962; 5 febbraio 1963-14 aprile 1963; 8 ottobre 1963-26 gennaio 1964.

La velocità radiale delle righe dello spettro shell indica che lo shell attraversa una fase di contrazione, e che la velocità di contrazione sta decrescendo dal '61 al '64. Si osserva anche una stratificazione nello shell; le parti più esterne dove sono formate le righe di Balmer (e cioè ad un'altezza di circa tre raggi stellari) si contraggono ad una velocità inferiore a quella degli strati in cui sono formate le righe metalliche (e cioè ad un'altezza di circa due raggi stellari). Si osservano apprezzabili variazioni anche a distanza di pochi giorni nei profili in emissione di Hα e nel valore della discontinuità di Balmer. Il numero di righe di Balmer visibili è aumentato da H 28 (1961) ad H 36 (1964).

Si trova che il rapporto H/He nell'atmosfera di ζ Tauri è circa 2 o 3 volte inferiore a quello osservato nelle stelle normali.

La curva di crescenza per le righe del Fe II è confrontata con quella di α Cygni.

Abstract. — The results of the spectrographic observations of ζ Tauri are given. This star was observed during the following three epochs: Nov. 16, 1961-March 26, 1962; Febr. 5, 1963-Apr. 14, 1963; Oct. 8, 1963-Jan. 26, 1964. The radial velocity of the shell lines indicates that the shell undergoes a contraction phase and the contraction velocity is decreasing from 1961 to 1964. We have also found evidence of stratification: the outer parts of the shell, where the Balmer lines are formed (at a height of about three stellar radii) the shell is contracting at a lower velocity than the lower parts where the metallic lines are formed (at a height of about two stellar radii). We have observed appreciable variations at intervals of few days in the emission contours of Hα and in the value of the Balmer discontinuity. The number of visible Balmer lines is increased from H 28 (1961) to H 36 (1964).

The ratio H/He in the stellar atmosphere is about two or three times lower than that observed in normal stellar atmospheres.

The curve of growth for the shell Fe II lines has been compared with the curve of growth for α Cygni.

(*) On leave of absence from the Astronomical Institute of Ankara (Turkey).
(**) Ricevuta il 22 febbraio 1965.

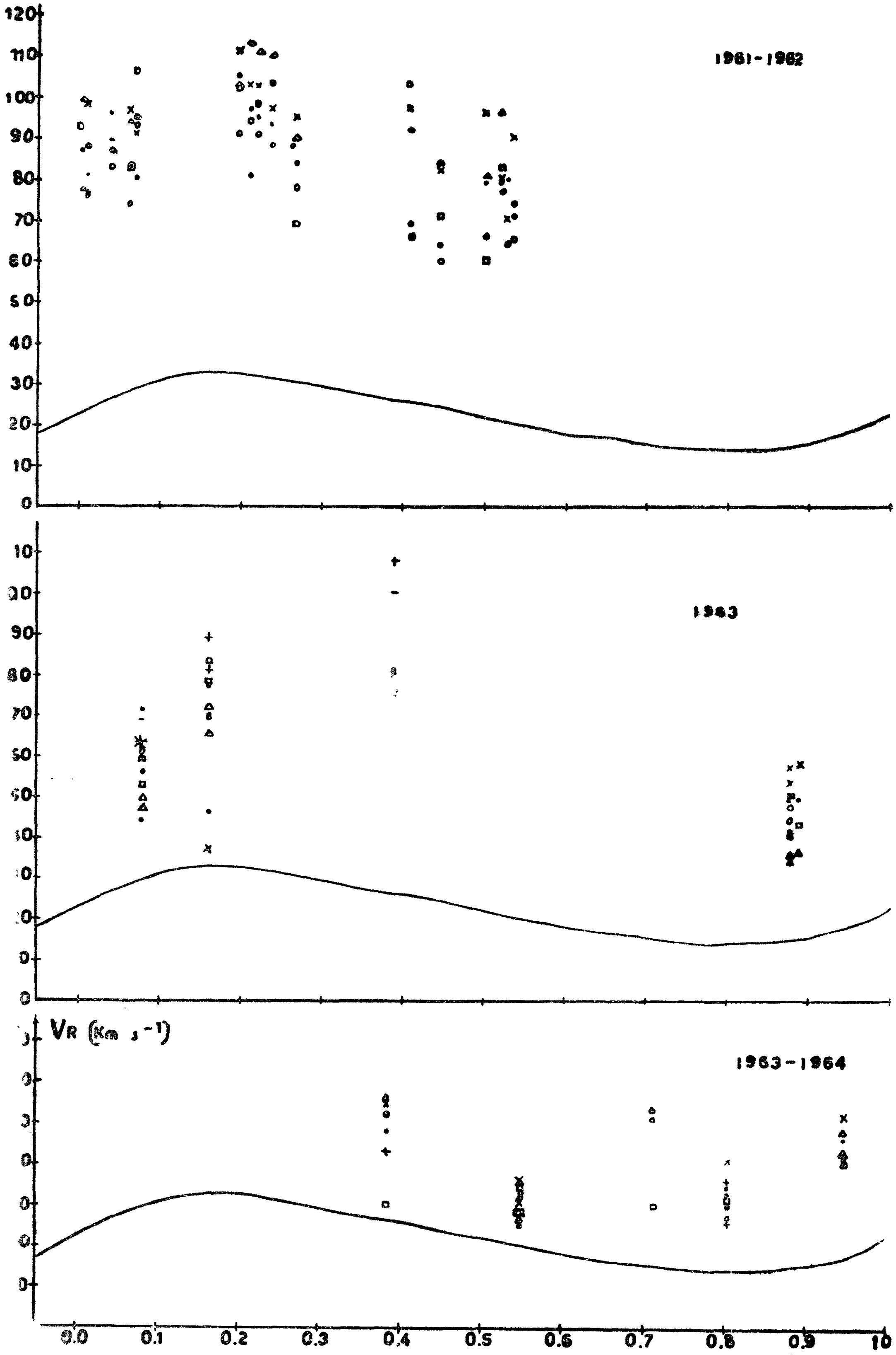

Fig. 1 - Radial velocities of the shell lines:
○ H I; × Mg I; □ Fe II; △ Si II; ● Ca II; + Ni II; – Cr II.

Several spectrograms of ζ Tauri have been obtained with the grating spectrograph of the Merate Observatory from November 1961 to January 1964 (Table I).

The spectrograms have been measured for the determination of the radial velocity, and microphotometric tracings have been obtained for the measurements of the intensity of the absorption and emission lines.

RADIAL VELOCITY OF THE SHELL

The radial velocity given by the shell lines (hydrogen line cores and metallic lines) indicate that the shell is contracting and that the contraction velocity is decreasing from 1961 to 1964.

Hence, after the expansion period observed in 1958-59 (1) and the quiescent period of 1960 (2), a new phase of contraction has been found. It is therefore necessary to observe this star continuously for several years to detect if these expansion and contraction phases of the shell present some regular recurrency or are completely irregular.

In a preliminary note (3) we have remarked that during the period 1961-1962 a systematic difference between the radial velocity given by the hydrogen line, by the Fe II and Ca II lines and by the Si II and Mg I lines exists. This difference suggests a stratification in the shell, the outer parts of which, where the Balmer lines are formed, are contracting with a lower velocity than the internal parts of the shell. This systematic difference has practically disappeared at the third epoch of these observations (Oct. 1963-Jan. 1964) (see Table II and Fig. 1).

LINE IDENTIFICATIONS AND INTENSITY VARIATIONS

Table III gives the identifications and the average equivalent widths for the three epochs: winter 1961-62; winter-spring 1963; winter 1963-64.

No appreciable variations of intensity are found. The most important variation consists in the increase of the number of visible Balmer lines from H 28 in 1962 to H 36 in 1964. A slight increase in the emission wings of the Fe II lines is found from 1963 to 1964.

A comparison with the results of previous observations shows that the Fe II shell lines reach a maximum in 1958, a minimum in the fall of 1960

TABLE I

Sp. No.	Date	J.D.	Phase	Spectral Range
900	11/16/61	2437620.48	164.521	3400 — 4300 III order
910	12/17/61	621.46	.528	»
914	12/18/61	622.42	.536	»
922	1/19/62	684.42	165.002	»
928	1/20/62	685.42	.004	»
939	1/24/62	689.35	.039	»
952	1/27/62	692.37	.062	»
957	1/28/62	693.32	.069	»
960	2/14/62	710.28	.196	»
963	2/16/62	712.32	.212	»
970	2/17/62	713.28	.219	»
978	2/19/62	715.80	.238	»
984	2/21/62	717.84	.253	»
986	2/23/62	719.76	.268	»
992	3/14/62	738.33	.408	»
1027	3/19/62	743.29	.445	»
1044	3/26/62	750.84	.502	»
1622	2/ 5/63	2438066.39	167.876	3300 — 4600 II order
1623	2/ 5/63	066.93	.876	»
1632	2/ 6/63	067.42	.884	»
1644	3/ 4/63	093.29	168.078	»
1645	3/ 4/63	093.30	.078	»
1662	3/15/63	104.31	.161	»
1663	3/15/63	104.32	.161	»
1672	4/14/63	134.33	.387	»
1845	10/ 8/63	310.58	169.713	5700 — 7000 II order
1846	10/ 8/63	310.59	.713	4500 — 5800 II order
1847	10/ 8/63	310.60	.713	3300 — 4600 II order
1871	10/27/63	329.60	.856	3400 — 4300 III order
1872	10/27/63	329.61	.856	»
1873	10/27/63	329.62	.856	3300 — 4600 II order
1874	10/27/63	329.63	.856	»
1875	10/27/63	329.64	.856	4500 — 5800 II order
1876	10/27/63	329.65	.857	5700 — 7000 II order
1895	11/ 8/63	341.53	.946	3400 — 4300 III order
1896	11/ 8/63	341.535	.946	3300 — 4600 II order
1897	11/ 8/63	341.544	.946	4500 — 5800 II order
1898	11/ 8/63	341.560	.946	5700 — 7000 II order
1932	1/ 4/64	399.50	170.382	3400 — 4300 III order
1933	1/ 5/64	399.52	.382	5700 — 7000 II order
1934	1/ 5/64	399.53	.382	4500 — 5800 II order
1935	1/ 5/64	399.54	.382	3300 — 4600 II order
1960	1/26/64	421.35	.547	3400 — 4300 III order
1961	1/26/64	421.37	.547	»
1962	1/26/64	421.38	.547	3300 — 4600 II order
1963	1/26/64	421.38	.547	»
1964	1/26/64	421.39	.547	4500 — 5800 II order
1965	1/26/64	421.43	.547	5700 — 7000 II order

TABLE II

Sp. No.	HI	FeII	CaII	SiII	MgI	NiII	MgII
Radial Velocities (Km/sec) Nov. 1961 - Mar. 1962							
900	77±3	83± 4	79	91± 8	84± 9		
910	64±3	71±17	80	89±	70± 7		
914	74±2	65± 3	71		90± 4		
922	78±3	93± 7	88	99± 2	92± 2		
928	77±2	76± 3	81	88± 7	98± 3		
939	83±2	89± 1	96	87± 5			
952	74±2	83± 2	83	94± 3	97± 4		
957	93±6	106± 6	80	95± 4	91± 3		
960	91±9	102±20	103	103±10	111± 1		
963	97±3	94± 5	81	113± 7	103±10		
970	91±3	98± 8	95	111± 5	103± 9		
978	88±3	103± 5	93	110± 7	84± 8		
984	83±3		78	115±12	123±10		
986	78±1	69± 6	84	90± 1	95± 8		
992	69±2	103± 7	66	92± 3	97±10		
1027	60±2	71± 3	64	84±10	82± 9		
1044	66±3	60±10	79	81± 7	96± 4		
Mean	79	85	82	96	95		
Radial Velocities (Km/sec) Feb. 1963 - Apr. 1963							
1622	47±2	50± 6	49	35± 9	57± 9	—	—
1623	44±2	40± 4	41	34	53	—	40
1632	58±2	43± 5	49	36± 7	58± 3	—	45
1644	61±1	53± 3	71	47± 4	63± 9	59±10	50
1645	56±1	69± 3	44	49± 3	—	63± 5	62
1662	70±4	83± 4	46	72±15	—	89	83
1663	69±3	78± 9	77	65±13	37	81	62
1672	80±2	75± 2	81	73± 9	75±10	108	64
Mean	61	61	57	51	57	80	58
Radial Velocities (Km/sec) Oct. 1963 - Jan. 1964							
1847	51±3	30± 3	52	53± 1	31		23
1872	30±1	—	35	31± 3	41± 2	26± 1	—
1873	29±5	33± 4	—	—	—	—	—
1874	27±2	31± 3	33	28± 8	31± 0	36	14
1895	43±3	—	46	48± 7	52± 3	—	—
1896	40±3	42± 2	40	43± 4	—	29	19
1932	47±1	38± 4	41	41± 1	39± 3	31± 8	—
1935	52±2	30± 3	48	56±10	55± 2	43	20
1960	33±1	30± 4	28	28± 2	36± 2	24	—
1961	32±1	28± 3	31	27± 2	31± 3	—	—
1962	24±3	34± 4	27	36± 3	42	38	17
Mean	37	33	35	39	40	32	19

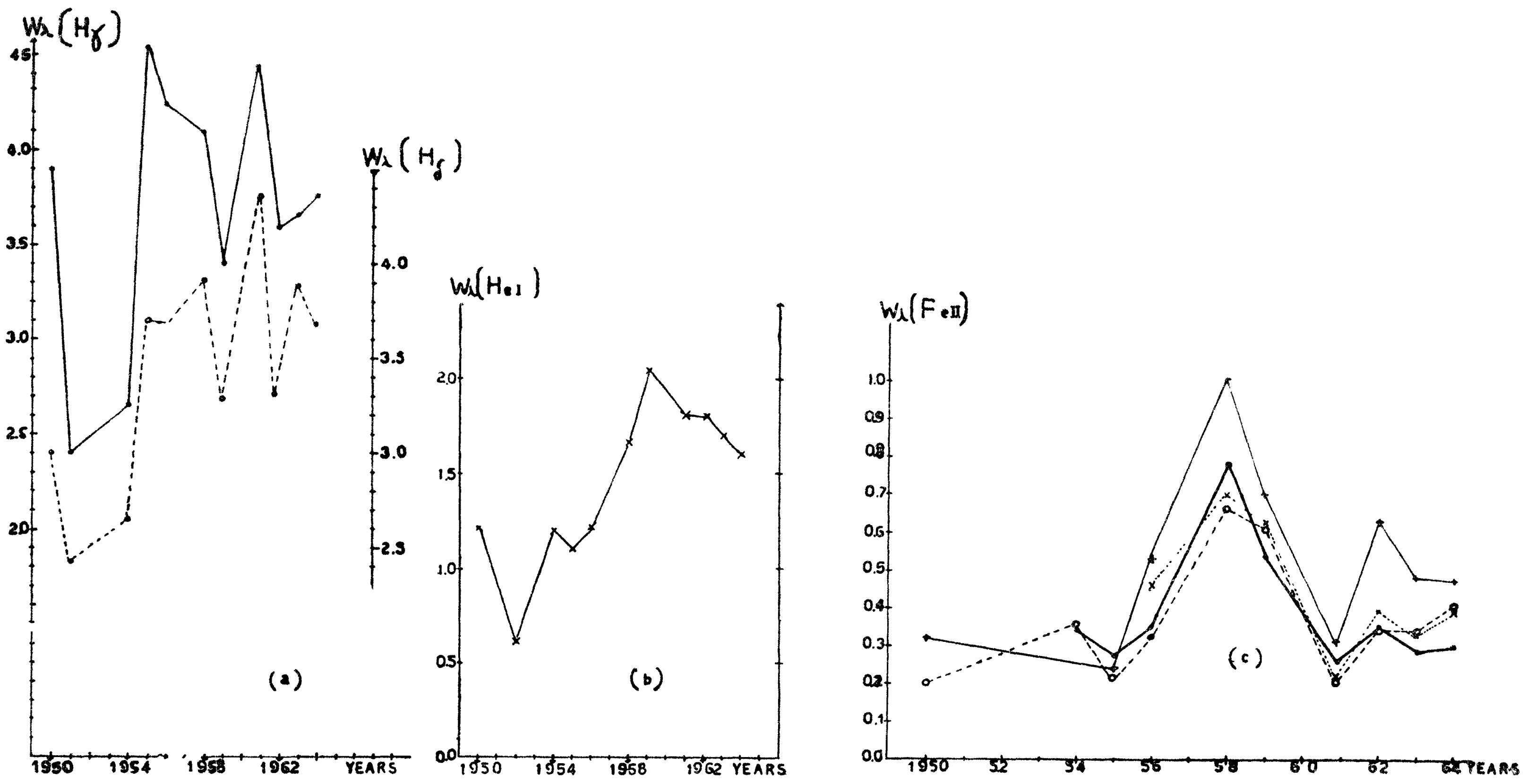

Fig. 2 - (*a*) Intensity variations of Hγ (● ———) and Hδ (○ – – – –)
(*b*) Intensity variations of the He I lines. The equivalent width W is the mean of the equivalent widths of $\lambda\lambda$ 4471, 4388, 4144, 4026, 4009.
(*c*) Intensity variations of the Fe II shell lines: + λ 4351; × λ 4233; ○ λ 4178; ● λ 4173.

TABLE III

λ		Identification	Wλ	Wλ	Wλ
3465.62		Ni II (4)			
3468.680		Fe II (114)			
3471.75		Ni II (4)			
3493.468		Fe II (114)			
3513.93		Ni II (1)			
3554.394		He I (34)			
524					
3576.762		Ni II (4)			
3587.257		He I (31)			
396					
3608 314					
3613.641		He I (6)			
3634.235		He I (28)			
373					
3643.677					
3657.926		H 35			0.04
3658.641		H 34			0.05
3659.423		H 33			0.07
3660.279		H 32			0.08
3661.221		H 31			0.10
3662.258		H 30			0.13
3663.406		H 29			0.17
3664.679		H 28			0.20
3666.097		H 27			0.23
3667.684		H 26			0.30
3669.466		H 25			0.37
3671.478		H 24	0.30		0.40
3673.761		H 23	0.32		0.45
3676.365		H 22	0.41		0.53
3677.69					
86	bl.	Cr II (12)			
93					
3679.355		H 21	0.45	0.56	0.60
3682.810		H 20	0.48	0.60	0.69
3685.192		Ti II (14)			
3686.833		H 19	0.40	0.53	0.78
3691.557		H 18	0.50	0.63	0.81
3694.231					
3697.154		H 17	1.00	0.61	1.13
3703.855		H 16			
3706.219		Ti II (73)			
3711.973		H 15	1.20	1.30	1.32
3715.19		Cr II (2)			
45		Cr II (145)			
476		V II (15)?			
3719.935		Fe I (5)			
3721.940		H 14	1.57	1.70	1.34
3725.304	bl.	Fe II (130)	0.04	0.09	0.11
901		Fe II			
3727.37		Cr II (117)			
33	bl.	O II (3)	0.13	0.08	0.15
351		V II (21)?			
3729.34			0.07		0.04

Table III (continued)

λ	Identification	Wλ	Wλ	Wλ
3731.122				
3734.370	H 13	1.83	2.05	1.79
3738.38	Cr II (20)			
3741.633	Ti II (72)	0.10	0.09	0.09
3745.561 bl.	Fe I (5)			0.08
806	V II (15)			
3749.49 bl.	O II (3)			
487	Fe I (21)			
3750.154	H 12	2.41	2.20	2.20
3754.59	Cr II (20)			
3755.563	Fe II (154)	0.08		0.06
3757.684	Ti II (72)			0.04
3759.291 bl.	Ti II (13)	0.38	0.26	0.25
460	Fe II			
3761.320 bl.	Ti II (13)			
866	Ti II (107)	0.16		0.14
90	Cr II (11)			
69				
3762.894 bl.	Fe II (192)			
63	O II (31)			0.16
3763.790	Fe I (21)			0.08
3769.455	Ni II (4)			
3770.632	H 11	2.41	3.40	2.78
3776.062	Ti II (72)			
3780.300				
3783.347	Fe II (14)	0.15	0.17	0.16
3797.900	H 10	3.09	3.42	3.28
3805.765	He I (63)			
3814.121	Fe II (153)	0.06	0.20	0.10
3819.606	He I (22)	1.71	1.66	1.47
3824.913	Fe II (29)	0.19	0.15	0.13
3829.3549	Mg I (3)	0.13	0.20	0.10
3832.2996	Mg I (3)	0.16	0.21	0.20
3037				
3835.386	H 9	3.66	3.61 (3.33)	3.64
3838.2918	Mg I (3)	0.26	0.20	0.27
2943				
3845.181				
3849.58 bl.	Ni II (11)	0.18	0.22	0.20
8.24	Mg II (5)			
3853.657	Si II (1)		0.11	0.15
3856.021	Si II (1)	0.27	0.39	0.28
3862.592	Si II (1)	0.22	0.31	0.25
3865.59 bl.	Cr II (167)			
6.01	Cr II (130)			
6.54				
3871.819	He I (60)	1.45		0.88
3878.180	He I (59)			
3889.051 bl.	H 8			
8.646	He I (2)			
3891.981				
3900.546	Ti II (34)	0.25	0.15	0.15

Table III (continued)

λ		Identification	W_λ	W_λ	W_λ
3905.64	bl.	Cr II (167)	0.15	0.15	0.21
6.037		Fe II (173)			
3911.96		O II (17)			
2.088					
3913.464		Ti II (34)	0.26		0.09
4.480		Fe II (3)			
3926.530		He I (58)		0.83	0.95
3933.664		Ca II (1)	0.73	0.68	0.55
3935.914		He I (57)			
3935.942		Fe II (173)			0.14
3938.289	bl.	Fe II (3)	0.25	0.15	0.15
969		Fe II (190)			
3945.048		O II (6)			
3947.301					
489		O I (3)	0.22	0.22	0.21
584					
3954.372	bl.	O II (6)			0.12
5.851		N II (6)			
3960.895		Fe II (212)	0.16	0.12	0.12
3964.727		He I (5)	0.19		0.18
3970.074	bl.	H ε			
3968.470		Ca II (1)			
3974.160	bl.	Fe II (29)			
5.029		Fe II (191)			
3982.719		O II (6)			0.17
3994.996		N II (12)	0.92		0.51
4002.073	bl.	Fe II (29)	0.22		0.18
.549		Fe II (190)			
4009.270		He I (55)	1.91	1.63	1.33
4015.50		Ni II (12)	0.13	0.11	0.12
4026.189		He I (18)	2.24	1.89	1.68
382					
4041.321	bl.	N II (39)			0.53
3.537		N II (39)			
4057.457		Fe II (212)			0.16
4067.051		Ni II (11)	0.30	0.25	0.22
4069.897	bl.	O II (10)			
636					
4072.164		O II (10)			
4075.868	bl.	O II (10)			
45		Si II			
4098.957					
4101.737		H δ	3.31	3.89 (3.89)	3.69
4104.743	bl.	O II (20)			
5.000					
4120.812		He I (16)	1.41	1.55	1.08
993					
4122.638		Fe II (28)			0.11
4128.055	bl.	Si II (3)	0.33	0.34	0.28
735		Fe II (27)			
4130.884		Si II (3)	0.43	0.40	0.35
4143.76		He I (56)	1.39		1.38
4173.450		Fe II (27)	0.34	0.29	0.30

Table III (continued)

λ	Identification	W_λ	W_λ	W_λ
4178.855	Fe II (28)	0.33	0.34	0.41
4182.467				
4224				
4233.167	Fe II (27)	0.38	0.33	0.39
4236.968				
4246.829	Sc II (7)			0.14
4258.155	Fe II (28)			0.18
4296.567	Fe II (28)			0.21
4303.166	Fe II (27)	0.28	0.30	0.25
4307				0.12
4325.77	O II (2)			
88 bl.	C II (28)		0.20	0.28
765	Fe I (42)			
4337.916	Ti II (20)			
4340.468	H γ	3.60	3.65	3.76
4351.764	Fe II (27)	0.63	0.48	0.47
4357.574	Fe II		0.29	0.25
4361.249 bl.	Fe II			
2.10	Ni II (9)			
4368.262 bl.	Fe II		0.37	0.23
9.404	Fe II (28)			
4385.381	Fe II (27)		0.18	0.24
4387.928	He I (51)	1.66	1.36	1.44
4395.031 bl.	Ti II (19)			
78	Fe III (4)			
4402.875	Fe II			0.18
4411.080	Ti II (115)			
4416.817	Fe II (27)		0.40	0.40
4419.59	Fe III (4)			
4427.675				
4430.95	Fe III (4)			
4431.626	Fe II (222)			
4449.663	Fe II (222)			
4451.545	Fe II		0.37	0.51
4455.258	Fe II		0.14	0.28
4461.468				
4468.493	Ti II (31)			
4471.477 bl.	He I (14)		1.93	2.18
688				
4481.129	Mg II (4)		0.71	0.72
327				
4489.185	Fe II (37)			
4491.401	Fe II (37)			
4501.201	Ti II (31)		0.21	0.22
4508.283	Fe II (38)		0.39	0.38
4515.337	Fe II (37)		0.30	0.40
4520.225	Fe II (37)		0.22	0.30
4522.63	Fe II (38)		0.39	0.39
4533.966	Ti II (50)			
4534.166	Fe II (37)			
4541.523	Fe II (38)		0.22	0.23
4549.47 bl.	Fe II (38)		0.31	0.56
62	Ti II (82)			

Table III (*continued*)

λ	Identification	W_λ	W_λ	W_λ
4555.890 bl.	Fe II (37)		0.31	0.42
02	Cr II (44)			
4558.659	Cr II (44)			
4563.761	Ti II (50)			
4582.84 bl.	Fe II (37)			
3.83	Fe II (38)			0.41
4629.336	Fe II (37)			0.26
4713.143	He I (12)			
373				
4773.332				
4848				
4861.332	H β			
4870.121				
4883.415				
4890.821				
4921.929	He I (48)			
4923.921	Fe II (42)			0.65
4948.848	Fe II			
4967.92				
5015.675	He I (4)			0.34
5018.434	Fe II (42)			0.52
5022.874	Fe II			0.20
5026.234				
5047.736	He I (47)			
5100.704 bl.	Fe II			
706	Fe III			
840	Fe II (185)			
95	Fe II			
1.48	Fe II			
5127.32 bl.	Fe III (5)			
.866	Fe II (167)			0.80
5156.10 bl.	Fe II			
.0	Fe III (5)			0.33
5167.3216	Mg I (2)			
5169.030	Fe II (42)			0.50
5172.6843	Mg I (2)			0.17
5183.6042	Mg I (2)			0.42
5197.569	Fe II (49)			0.26
5234.620	Fe II (49)			0.27
5264.801	Fe II (48)			0.17
5272.413	Fe II (185)			0.28
5275.994	Fe II (49)			0.32
5316.609 bl.	Fe II (49)			0.36
777	Fe II (48)			
5325.559	Fe II (49)			
5362.864	Fe II (48)			
5682.953				
5743.753				
5835.61	Fe II			
5865.153				

Table III (*continued*)

λ	Identification	W_λ	W_λ	W_λ
5875.618 650 bl. 989	He I (11)			1.57
5889.953	Na I (1)			0.85
5891.36	Fe II (211)			
5895.923	Na I (1)			0.67
5967	atm.			
5991.383	Fe II (46)			
6149.238	Fe II (74)			
6191.091				
6238.375	Fe II (74)			0.20
6247.562	Fe II (74)			0.26
6277	atm.			
6305.318	Fe II (200)			0.10
6317	atm.			
6347.091	Si II (2)			0.60
6371.359	Si II (2)			0.42
6383.753	Fe II			
6416.905	Fe II (74)			
6456.376	Fe II (74)			0.32
6462	atm.			
6471	atm.			
6473.910				
6481.800				
6522	atm.			
6562.817	Hα			

Note to Table III: the third column gives the mean value of W_λ for the first epoch, the fourth column for the second epoch and the fifth column for the third epoch.

and increase again in 1962. From 1962 to 1964 there are only slight variations (Fig. 2). The variations of the Balmer lines (Hγ and Hδ) are shown in Fig. 2. Fig. 3 gives the contours of Hα and Hβ; observations of these spectral regions were available only for the third epoch. We can see that the variation of the shape of the emission contours is not very strong, but the intensity changes appreciably at intervals of a few days. The ratio V/R of the equivalent widths of the emission wings of Hα is of the order of unity, while the central intensities of the wings give V/R $>$ 1. The ratio V/R of the equivalent widths of the emission wings of Hβ is equal to 2.

The variation of the ratio V/R for Hβ is given in Fig. 4. From a long series of observations it appear that this ratio is appreciably different from unity when the shell spectrum is strengthened. Since the variation of the

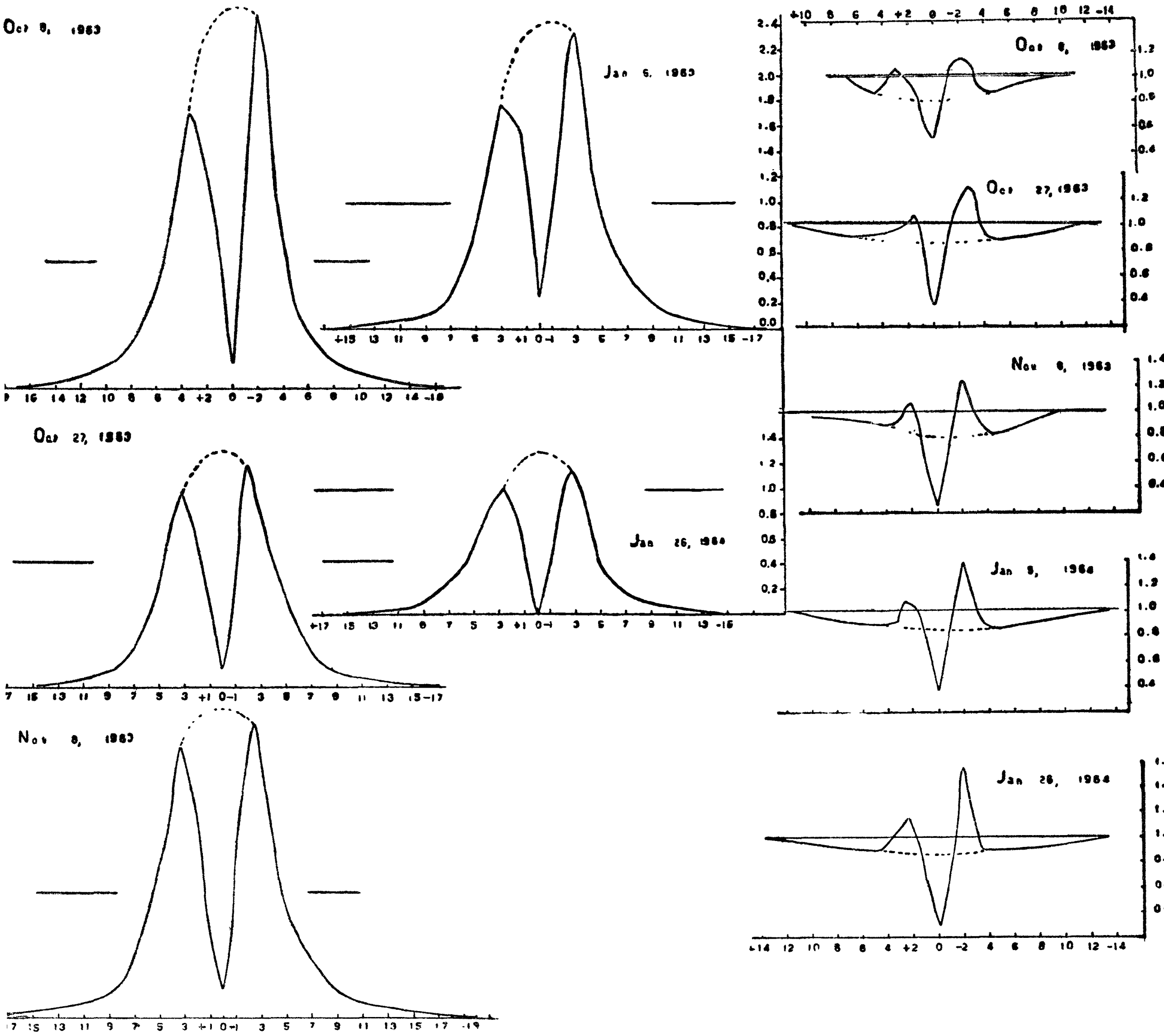

Fig. 3 - Contours of Hα (left); contours of Hβ (right).

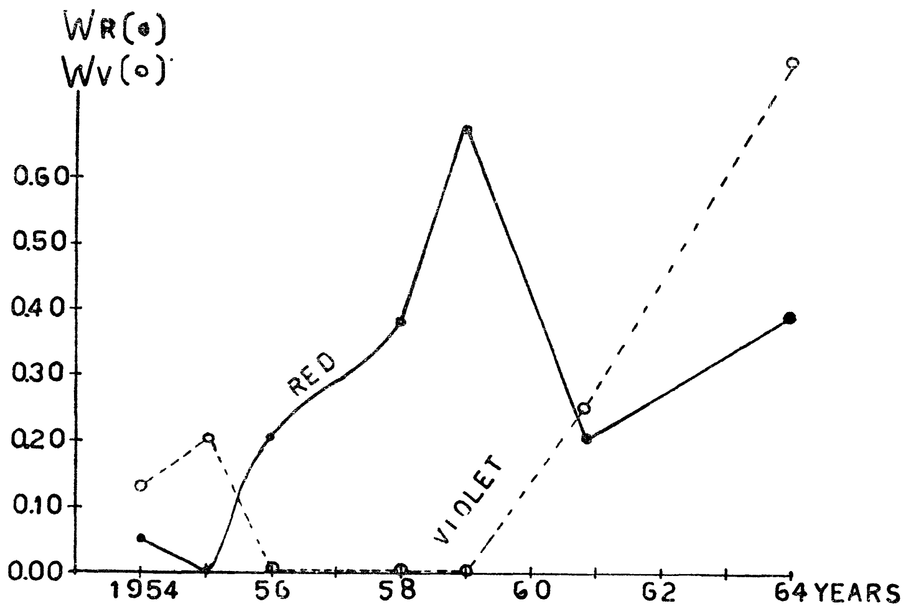

Fig. 4 - Intensity variations of the emission wings of Hβ

V/R ratio is mainly due to the violet-shift or to the red-shift of the absorption core, this behavior suggest that strengthening of the shell spectrum is usually associated with an expansional or a contractional phase of the shell, while when the shell is quiescent, and the emission wings are symmetrical with respect to the absorption lines, the shell spectrum is usually weak.

The emission wings of Hγ and Hδ are very weak; they are slightly stronger at the second epoch of this series of observations and have $V/R > 1$.

The Balmer discontinuity and the quantum number of the last resolved Balmer line are given in Table IV. Some variations appear to be real. The average value of D is equal to 0.25 ± 0.02 and is appreciably higher than the value given by Barbier and Chalonge (D = 0.18) (4). However, after reduction to the new series of measurements of 1948 (5) by Chalonge and Divan, we find D = 0.23, in good agreement with the mean value given by our spectrograms. The very low discontinuity observed on spectrogram 960 (Febr. 14, 1962), D = 0.07, and which is certainly lower than 0.12 and the high discontinuity observed on spectrogram 1672 (Apr. 14, 1963), D = 0.42 and which is certainly higher than 0.35, indicates that strong variations in the ionization degree of the shell can occur at intervals of a few days.

The variations of the quantum number n are partly imputable to the different dispersions which have been used. In fact the observations for the third epoch have been made partly in the second order, partly in the third

TABLE IV

Sp. No.	Grating Order	D	n
960	III	0.07 (<0.12)	H 28
978	III	0.19	H 24
1622	II	0.25	H 28
1623	II		H 28
1632	II	0.185	H 27
1644	II	0.19	H 29
1645	II	0.24	H 29
1672	II	0.42 (>0.35)	H 30
1847	II	0.26	H 28
1872	III	0.215	H 35
1874	II	0.24	H 30
1895	III	0.185	H 34
1896	II	0.23	H 27
1932	III	0.20	H 35
1960	III	0.25	H 36
1961	III	0.24	H 35

order, and the first ones give systematically lower values for *n* than the second ones. However the variation from $n = 28$ to $n = 36$ from the first to the third epoch is very probably real, since the same dispersion of 23 A/mm has been used.

THE HYDROGEN AND HELIUM ABUNDANCE IN THE STELLAR ATMOSPHERE

The number of atoms of hydrogen and helium present in a column of a height equal to the total height of the stellar atmosphere and the shell has been computed. For hydrogen we have used the Unsöld method (6) which gives a lower limit:

$$\log N_{0,2}\, h \geq 16.12$$

A better approximation is given by the Minnaert formula which gives:

$$\log N_{0,2}\, h = 16.76$$

(with $R_c = 0.85$ and $R = 1 - 10^{-D} = 0.41$).

The electron density computed by means of the Inglis and Teller formula

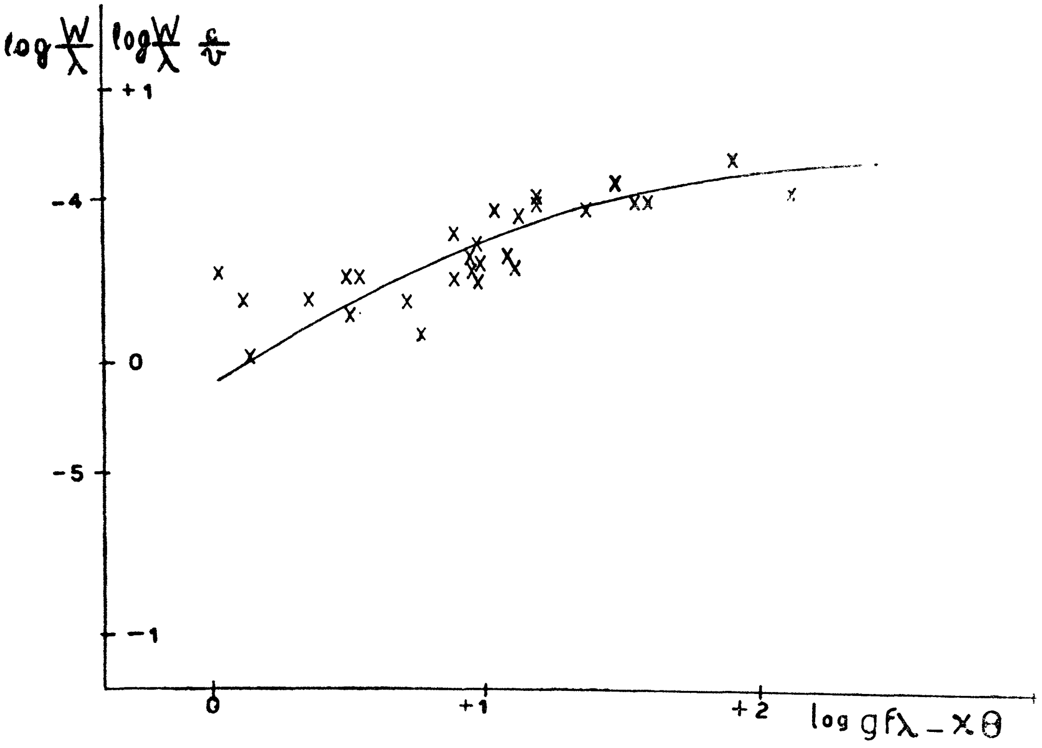

Fig. 5 - Curve of growth for the Fe II shell lines.

gives a value which represents the physical conditions in the shell. In fact the last visible Balmer lines are shell cores. We find

$$\log N_e = 11.68 \quad \text{for } n = 36$$
$$\log N_e = 12.36 \quad \text{for } n = 28$$

The Holtsmark method, which depends from the equivalent widths of Hγ and Hδ, gives, on the contrary, a value which represents better the electron density in the stellar atmosphere. In fact the contribution that the shell core gives to the total intensity of the line is rathers mall. We find

$$\log N_e = 13.38 \quad (H\gamma)$$
$$\log N_e = 13.43 \quad (H\delta)$$

The helium abundance has been derived by means of the Unsöld method, which gives

$$\log N_{0,2^3P}\, h \geqq 15.70$$

Another value of log $N_{0,2^3P}$ h has been found using the method of the curve of growth, assuming that the Stark effect has a negligible effect on the line contours. We find the following results: from the vertical shift given to the empirical curve in order to match the theoretical curve

$$\log\sqrt{\frac{2\,k\,T}{\mu}+\xi^2} - \log\sqrt{\frac{2\,k\,T}{\mu}} = 0.45$$

and assuming T = 18000 °K, ξ = 20 km/s.

From the horizontal shift we find log $N_{0,2^3P}$ h = 15.95, a value which is in good agreement with the lower limit given by the Unsöld method.

The total abundances of hydrogen and helium have been computed using values of the electron pressure and temperature representing the physical conditions of the stellar atmosphere. Since ζ Tauri is a B3 star, we compute the abundances for the two values of the temperature T = 18000 and T = 15000 °K (7), and log P_e = 1.75 (which follows from log N_e = 13.4). We find:

for T = 15 000	log Nh (H I) = 19.57	,	log Nh (He I) = 22.01	
	log Nh (H II) = 23.23	,	log Nh (He II) = 22.60	
for T = 18 000	log Nh (H I) = 19.00	,	log Nh (He I) = 20.84	
	log Nh (H II) = 23.62	,	log Nh (He II) = 23.00	
log Nh (H) = 23.23	(for T = 15 000)	;	log Nh (H) = 23.62	(for T = 18 000)
log Nh (He) = 22.70	» »	;	log Nh (He) = 23.00	» »
log H/He = +0.53	(T = 15 000)	;	log H/He = +0.62	(T = 18 000)

The ratio H/He has been computed also using the method suggested by Unsöld (6), and consisting in the direct comparison of the equivalent widths of Hγ and λ 4471, and of Hδ and λ 4026. This method can be used only if both hydrogen and helium are almost completely ionized once, and therefore only if the temperature in the atmosphere of ζ Tauri is greater than 15000 °K. This method has the advantage of depending only slightly upon the temperature. We find

$$\log H/He = -0.16 \quad (H\gamma \text{ and } 4471)$$
$$\log H/He = +0.16 \quad (H\delta \text{ and } 4026)$$

It seems probable that helium is sligthly in excess, in comparison with the majority of the normal stars, where log H/He is included in the range between 0.7 and 1.0. By the study of several high dispersion spectrograms obtained in the last months of 1960 (2) we have found log H/He = +0.35.

All these results, though rather unreliable for the uncertainty in the choice of the temperature, indicate a ratio H/He which is two or three times lower than the value found in the normal stellar atmospheres. We therefore conclude that probably the atmosphere of ζ Tauri is slightly hydrogen-poor.

CURVE OF GROWTH OF THE FeII LINES OF THE SHELL

Several sharp and strong lines of Fe II are present in the shell spectrum and make possible a direct estimate of the physical conditions of the shell. The curve of growth for these lines has been constructed using the values of log gfλ given by H.G. Groth (^{8}). This curve has been compared with the Fe II curve of growth for α Cygni (^{8}).

The physical conditions in the atmosphere of an A2 I_a star are probably very similar to those in the shell of ζ Tauri. This makes α Cygni a very suitable standard star. The results are the following ones:

$$\log c/v\ (\alpha \text{ Cygni}) = \log c/v\ \ (\zeta \text{ Tauri}) = 4.60$$

and therefore $v = 7.6$ km/s.

From the horizontal shift between the two curves of growth it follows that

$$\log X\zeta - \log X\alpha = +0.10$$

and therefore

$$\log Nh\zeta - \log Nh\alpha = \log X\zeta - \log X\alpha + \log v\zeta - \log v\alpha + \chi_{rs}\,(\theta\zeta - \theta\alpha)$$

We have no possibility of deriving directly the value of the excitation temperature in the shell. We can only infer that it is probably much lower than the atmospherical temperature and rather close to that of an A-type star. Assuming $\theta\zeta = 0.50$ and $\theta\alpha = 0.53$ (^{8}) we have

$$\text{Log } Nh\zeta - \log Nh\alpha = +0.02$$

For the total abundance we have (using $\log N_e = 11.7$)

$$\log Nh\zeta - \log Nh\alpha = 1.21$$

Assuming that the two stars have the same iron abundance, this result indicates that the optical depth in the shell atmosphere of ζ Tauri is 16 times lower than that in the atmosphere of α Cygni.

TABLE V

λ	multiplet	$-\log \frac{W}{\lambda}$	$\log\, g f \lambda$
4173.450	Fe II (27)	4.13	0.89
4233.167	Fe II (27)	4.03	1.55
4303.166	Fe II (27)	4.23	0.95
4351.764	Fe II (27)	3.96	1.48
4385.381	Fe II (27)	4.25	0.98
4416.817	Fe II (27)	4.04	0.90
4122.638	Fe II (28)	4.58	0.10
4178.855	Fe II (28)	4.01	1.20
4258.155	Fe II (28)	4.37	0.12
4296.567	Fe II (28)	4.30	0.50
4515.337	Fe II (37)	4.05	1.04
4520.225	Fe II (37)	4.17	0.97
4555.890	Fe II (37)	4.03	1.20
4583.83	Fe II (38)	4.04	1.60
4629.336	Fe II (37)	4.24	1.12
4508.283	Fe II (38)	4.07	1.13
4508.283	Fe II (38)	4.07	1.13
4522.63	Fe II (38)	4.06	1.36
4541.523	Fe II (38)	4.29	0.54
3783.347	Fe II (14)	4.37	0.14
3935.942	Fe II (173)	4.42	2.00
4057.457	Fe II (212)	4.40	
4923.921	Fe II (42)	3.88	1.98
5018.434	Fe II (42)		2.10
5169.030	Fe II (42)	4.01	2.21
5197.569	Fe II (49)	4.30	1.13
5234.620	Fe II (49)	4.28	1.20
5275.994	Fe II (49)	4.22	1.33
6238.375	Fe II (74)	4.50	1.38
6247.562	Fe II (74)	4.39	1.33
6456.374	Fe II (74)	4.31	1.59
5272.413	Fe II (185)	4.27	1.73

GEOMETRICAL DILUTION AND RADIUS OF THE SHELL

The geometrical dilution factor W is given by the relation (2)

$$W = 1/2 \left[1 - \sqrt{1 - (R/r)^2}\,\right]$$

where R is the stellar radius and r the radius of the shell at the height corresponding to which a given line is formed. Calling v_s and v the rotational velocities of the shell and the star, the broadening of the stellar lines gives us v, and the broadening of the shell lines gives $v_s' = v_s\ (R/r)$. Assuming that there is conservation of angular momentum we have $rv_s = Rv$ and finally $(R/r)^2 = v_s'/v$.

The values of v observed from the He I lines give v = 405 km/s. The

TABLE VI

Shell Lines	V_s'	Stellar Lines	V km/sec
3759 Ti II	93	3819 He I	382
3856 Si II	76	4009 He I	455
3862 Si II	76	4026 He I	419
4067 Ni II	70	4120 He I	388
4130 Si II	76	4143 He I	381
4173 Fe II	67		
4233 Fe II	58	Mean	405
4923 Fe II	97		
5018 Fe II	76		
5169 Fe II	72		
5316 Fe II	70		
Mean	76		

values of v_s' derived by the Fe II, Ti II, Ni II and Si II lines give $v_s' = 76$ km/s.

It follows that $W = 0.05$. For the ratio R/r at the height of which the metallic lines are formed we have $R/r = \sqrt{76/405} = 1/2.3$

The ratio R/r at the height at which the Balmer line cores are formed can be derived by comparing the rotational velocities given by the width of the emission contours of Hα and Hβ with the width of the absorption cores of Hα and Hβ. It follows that $R/r = v_s'/v_s = 0.31$ Hence the radius of the shell at the height at which the Balmer lines are formed is about three times the stellar radius, and at the height at which the metallic lines are formed it is about 2.3 times the stellar radius.

It follows that the mass of the shell (in the hypothesis of a spherical shell) is given by

$$\mathfrak{M} = 2\text{x } 10^{-9}\,\mathfrak{M}_\odot$$

(assuming $R = 3 \times 10^{11}$ cm $= 4.3\ R_\odot$, and $N_H = N_e = 10^{12}$ particles cm^{-3}).

REFERENCES

(1) A. Gökgöz, M. Hack, I. Kendir - Mem. S.A.I. **33**, 239, 1962

(2) A. Gökgöz, M. Hack, I. Kendir - Mem. S.A.I. **34**, 87, 1963

(3) M. Hack, C. Aydin, S. Islik - Mem. S.A.I. **35**, 331, 1964

(4) D. Barbier, D. Chalonge - Ann. Ap. **4**, 30, 1941

(5) D. Chalonge, L. Divan - Ann. Ap. **15**, 201, 1952

(6) A. Unsöld - Z. f. Ap. **21**, 22, 1941

(7) J.A. Hynek - *Astrophysics* - McGraw - Hill, New York, 1951, p. 20

(8) H.G. Groth - Z. f. Ap. **51**, 231, 1961